Article

JOURNAL OF COMPOSITE MATERIALS

Journal of Composite Materials
0(0) 1–14

DOI: 10.1177/0021998315601891
jcm.sagepub.com

SAGE

Synergistic effect of polyaniline, nanosilver, and carbon nanotube mixtures on the structure and properties of polyacrylonitrile composite nanofiber

Olcay Eren[1], Nuray Ucar[2], Aysen Onen[1], Nuray Kizildag[2] and Ismail Karacan[3]

Abstract

In this study, various amounts of carbon nanotubes (CNTs), nanosilver (AgNPs), and polyaniline (PANI) were incorporated at the same pot into the structure of composite polyacrylonitrile (PAN) nanofibers, which were produced by electrospinning process in order to see synergistic effect of the additives on the final properties of the composite materials. Performance and characteristic properties of composite nanofibers were analyzed by tensile tester, electrical conductivity meter, Fourier Transform Infrared Spectroscopy, differential scanning calorimetry, X-ray diffraction, scanning electron microscopy, and antimicrobial activity test. Statistical analysis (analysis of variance) was performed to see whether the differences were statistically significant or not. It was seen that samples with AgNPs had higher breaking strength and electrical conductivity than the samples with CNTs. Generally, PANI improved the crystallinity of the composite material more than the nanoparticles (CNTs and AgNPs). Even though each of the nanoparticles was used in low concentrations, the composite materials (PAN–1CNT–1$AgNO_3$–R and PAN–PANI–1$AgNO_3$–R) gained antimicrobial properties due to the synergistic effect of additives. The results suggested that PAN composite nanofibers with 3 wt% PANI and 1 wt% $AgNO_3$ generally presented better performance than the other samples in terms of electrical conductivity, antimicrobial activity, mechanical strength, crystallization, and thermal stability.

Keywords

Composite, electrospinning, functionalized carbon nanotube, nanofiber, polyacrylonitrile, polyaniline, synergistic effect, silver nanoparticles

Introduction

As it is known, polyacrylonitrile (PAN) is one of the most important polymers, which can have applications in textiles, automotive industry, drug applications, and implant materials in medical sector, membranes, etc.[1] Polyaniline (PANI) is also an important polymer, for example, doped PANI has electrical conductivity property.[2] Thus, polymer composites including PANI can be employed in many areas such as antistatic textiles, electromagnetic shielding, filtration media, sensors and actuators, and radiation detectors.[3–10] There are also many inorganic nanofillers available, which are used to improve the properties of polymer matrix. Carbon nanotubes (CNTs) have desirable properties including good mechanical, electrical, and thermal properties[11] and are reported to improve the mechanical properties when they are incorporated into the polymers.[12] CNTs are generally functionalized with carboxyl or amine groups to provide better interfacial bonding between polymer matrix and CNTs.[11,13] Besides, silver nanoparticles are also widely used in polymer composites. Various reduction methods exist

[1]Department of Polymer Science and Technology, Istanbul Technical University, Turkey
[2]Department of Textile Engineering, Istanbul Technical University, Turkey
[3]Department of Textile Engineering, Erciyes University, Turkey

Corresponding author:
Nuray Ucar, Textile Engineering Department, Istanbul Technical University, Inonu Caddesi, No: 65, 34437 Gumussuyu, Istanbul, Turkey.
Email: ucarnu@itu.edu.tr

for in situ synthesis of silver nanoparticles from silver nitrate ($AgNO_3$) such as chemical reduction by hydrazinium hydroxide (N_2H_5OH), reflux method, and exposure to light, which can affect the properties of the final material.[14] With the addition of silver nanoparticles, composites may have the potential to be used in wound-healing applications, filtering media, chemical and biological protective materials (biocidal agents against bacteria), air or water filters for purification purposes due to their good electrical conductivity, antimicrobial, reinforcing and catalyst properties.[13,15]

As seen from the published literature, there are many studies performed on composite nanofibers of PAN with CNTs and composite nanofibers of PAN with $AgNO_3$, but very limited number of studies on composite nanofibers of PAN with PANI. Qiao et al.[15] observed increases in diameter, E-modulus, and tensile strength by the addition of CNTs. Park et al.[16] investigated the effect of the functional groups of CNTs on PAN/CNT nanofibers and pointed out that the enthalpy of cyclization of the composites with the functional CNTs increased compared to pure PAN fibers. Wang et al.[17] pointed out that the mechanical properties improved with the addition of functionalized CNTs. Shi et al.[18] studied the properties of PAN/nanosilver (AgNPs) nanofibers and reported excellent antimicrobial activity with the incorporation of Ag nanoparticles. Sichani et al.[19] reported in situ preparation and characterization of PAN/AgNPs nanofibers. According to their research, polymer crystallinity increased with the addition of silver nanoparticles. When compared with the number of the studies that were performed on PAN/CNT and PAN/AgNPs composite nanofibers, there are very limited number of studies performed on PAN/PANI composite nanofibers,[7,20] which mainly focused on morphological properties, chemical structure, thermal properties, and structural properties. They had no information regarding the mechanical properties and conductivity of PAN/PANI composite nanofibers although PANI can have an important influence on the mechanical and electrical properties of composite nanofibers.

Besides, it still remains to be a question what the synergistic effect of the additives will be when they are used all together. As it is already known, improvement in mechanical properties is achieved by the incorporation of CNTs and $AgNO_3$; antimicrobial property is developed by the use of AgNPs; and electrical conductivity is improved by the use of PANI, CNT, and $AgNO_3$. Will it be possible to get more conductive and stronger composite material with antimicrobial properties when all the additives (CNT, $AgNO_3$, and PANI) are used together? In this study, for the first time, CNTs, $AgNO_3$, and PANI were used together in order to see their synergistic effect on the structure and properties of composite PAN nanofibers. While PANI content was kept constant as 3 wt%, the CNT and $AgNO_3$ contents were varied as 1 wt% and 3 wt%.

Experimental details

Materials

PAN (molecular weight of 150,000 g/mol), PANI (molecular weight of 65,000 g/mol), and camphorsulfonic acid (CSA, 232.3 g/mol) were purchased from Sigma Aldrich. Multi-walled CNTs (pristine, 60–100 nm in diameter, 5–15 μm in length) were purchased from NTP (China). They were amine-functionalized before use. Sulfuric acid (H_2SO_4), nitric acid (HNO_3), sodium nitrite ($NaNO_2$), isophorone diamine, *N,N′*-dimethylformamide (DMF) were used in the functionalization of the CNTs. $AgNO_3$ with 99.9995 % purity was purchased from Alfa Aesar Premion. Hydrazinium hydroxide (N_2H_5OH) was obtained from Merck. Dimethyl sulfoxide (DMSO) was used as the solvent in the preparation of the electrospinning solutions.

Methods

Amine functionalization of CNTs. Firstly, carboxyl functionalized CNTs (CNT–COOH) were synthesized according to Gao et al.'s method.[21] Then, amine functionalization was performed according to Zhao et al.'s method by using the CNT–COOH.[22]

Preparation of the solutions. A total of 7 wt% PAN was dissolved in DMSO to produce PAN-reference (PAN-ref) nanoweb. To make composite solutions of PAN—3 wt% PANI, required amount of PANI and CSA (equivalent molar ratio PANI:CSA = 1:2) were added to DMSO and mixed with magnetic stirrer at 40°C for two days. Then the solution was filtered with Sartorius Stedim filter paper (No.389).[23] For the preparation of PAN–CNT or PAN–$AgNO_3$ solutions, required amount of the additives (CNT–NH_2 or $AgNO_3$) were added to DMSO and the dispersions were homogenized with ultrasonic homogenizer (Bandelin Sonopuls HD 2070, probe type: KE76) for 10 min and then with ultrasonic bath for 45 min. Finally, PAN was added and the solutions were magnetically stirred at 40°C for 2.5 h until PAN was dissolved. For the preparation of PAN–PANI–CNT and PAN–PANI–$AgNO_3$ solutions, the additives of CNTs or $AgNO_3$ were added to the filtered PANI solutions and then the procedure for the PAN–CNT or PAN–$AgNO_3$ solutions was followed. The concentration of PANI was kept constant as 3 wt%, while the

Table 1. Codes of the samples produced.

Sample codes	Additives		
	CNT–NH_2	$AgNO_3$	PANI
PAN-ref	–	–	–
PAN–PANI	–	–	3%
PAN–1CNT	1%	–	–
PAN–3CNT	3%	–	–
PAN–PANI–1CNT	1%	–	3%
PAN–PANI–3CNT	3%	–	3%
PAN–1$AgNO_3$–R	–	1%	–
PAN–3$AgNO_3$–R	–	3%	–
PAN–PANI–1$AgNO_3$–R	–	1%	3%
PAN–PANI–3$AgNO_3$–R	–	3%	3%
PAN–1CNT–1$AgNO_3$–R	1%	1%	–
PAN–PANI–1CNT–1$AgNO_3$–R	1%	1%	3%

Note: CNT: carbon nanotube; PANI: polyaniline; $AgNO_3$: silver nitrate; PAN: polyacrylonitrile.

concentrations of CNTs and $AgNO_3$ were changed as 1 wt% and 3 wt% (with respect to the weight of PAN). The beakers that contained composite solutions with $AgNO_3$ were covered with aluminum foil to protect them from the negative effects of sunlight.

The composite samples were coded according to the additives used in their production. For example, nanoweb of PAN with 3 wt% PANI was coded as PAN–PANI, while nanoweb of PAN with 1 wt% CNT was coded as PAN–1CNT. The samples with AgNPs were coded as PAN–1$AgNO_3$–R and PAN–3$AgNO_3$–R with the additive amounts to be able to make a distinction between them although AgNPs were formed in the nanoweb structure after chemical reduction process. R was used to show that they were treated with the aqueous solution of hydrazinium hydroxide for the in situ synthesis of silver nanoparticles. The codes of the samples can be seen in Table 1.

Production of nanofibers by electrospinning. A high-voltage power supply was used to obtain an electric field in the electrospinning system. Polymer solution was loaded into a 10 ml syringe and then the solution was purged by the syringe pump to the needle tip. Grounded rotating drum collector was covered with aluminum foil. Nonwoven mat was covered on the aluminum foil. Polymer solution was drawn from needle tip due to the electric field and collected on the nonwoven mat as nanofiber web. The feeding rate of the solution was 1 ml/h, the applied voltage was 15 kV, and the distance between the needle tip and the collector was 10 cm (Figure 1). The nanowebs were produced under standard atmospheric conditions (temperature: $(20 \pm 2)^{\circ}$C, relative humidity: (65 ± 5)%) and were collected for 4 h.

In situ synthesis of silver nanoparticles. Chemical reduction by hydrazinium hydroxide was performed for the in situ synthesis of the silver nanoparticles. Composite nanofiber webs containing $AgNO_3$ were immersed into a solution of 20:1 v:v distilled water:hydrazinium hydroxide.[24] Then the nanowebs were washed two times with 100 ml distilled water and finally dried.

Characterization. Fungilab viscometer with R7 spindle was used to measure the viscosities of the solutions. Fourier Transform Infrared Spectroscopy (FTIR) spectra of functionalized CNTs, pure PAN, and PAN–PANI nanowebs were collected with Thermo Scientific Nicolet IS10 spectrometer. The scanning ranged from 4000 to 400 cm^{-1} with a signal resolution of 4 cm^{-1}. While KBr pellet method was used to collect the FTIR spectrum of CNT–NH_2, ATR method was used to collect the FTIR spectra of PAN-ref and PAN–PANI nanofibers. The morphology and the surface structure of composite nanofiber samples were investigated by scanning electron microscopy (SEM; Carl Zeiss EVO MA10). Image J Software was used to measure the diameters of nanofibers from SEM photomicrographs. At least 50 measurements were taken to obtain the average nanofiber diameters. Tensile tester with a 100 N load cell at a crosshead speed of 20 mm/min was used to measure the breaking strength and breaking elongation of nanofiber webs. The gage length was 15 mm. Specimens were cut in 35 mm (length) × 5 mm (width) dimensions for tensile testing. Mitutoyo digital micrometer was used to measure the thicknesses of the samples. At least seven measurements were performed to obtain the average values. Measurements were carried out at the standard atmospheric conditions. Microtest LCR Meter 6370 (with a measuring range of 0.01 mΩ–100 MΩ) with two circular probes and four wires was used for the measurement of the electrical resistances of composite nanofibers at standard atmospheric conditions. At least seven measurements were performed to obtain average values of volume resistance. The thicknesses of the samples were measured with an integrated thickness meter. Volume conductivity of the samples in S/cm were calculated using the formula indicated in ASTM standards.[25,26]

$$\gamma_v = t/(A \times R_v) \quad (1)$$

where γ_v is the electrical conductivity (S/cm), R_v is the volume resistance (Ω), A is the area of the electrodes (cm^2), and t is the distance between the electrodes (cm). Wide-angle X-ray diffraction (XRD) traces were

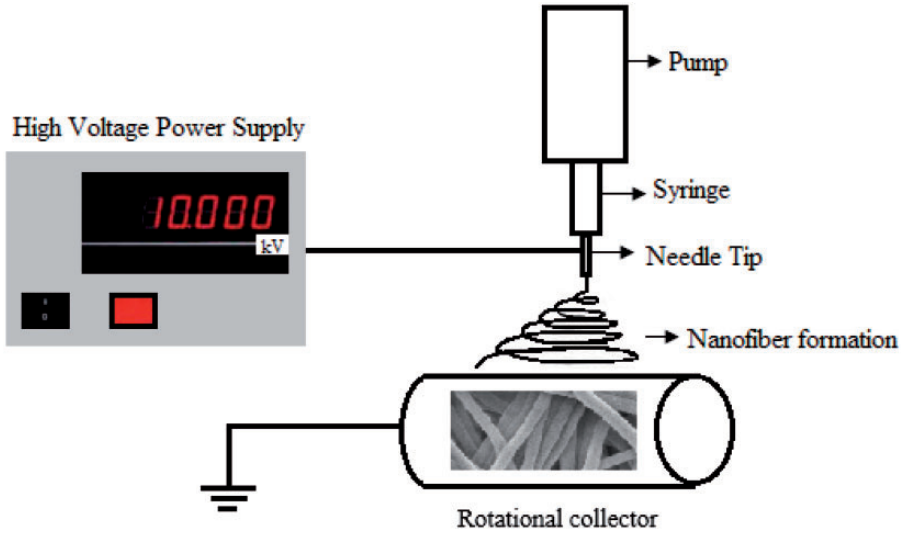

Figure 1. Scheme of electrospinning system.

obtained using a Bruker® AXS D8 Advance X-ray diffractometer system using nickel-filtered CuK_α radiation (λ, 0.15406 nm). The observed equatorial X-ray scattering data were collected in reflection mode in the 5–40° 2θ range. Apparent X-ray crystallinity is based on the ratio of the integrated intensity under the resolved peaks to the integrated intensity of the total scatter under the experimental trace.[27] Differential Scanning Calorimetry (DSC) Q10 was used for thermal analysis at a temperature range between 20°C and 350°C, at a heating rate of 20°C/min, under nitrogen atmosphere. Antimicrobial activity of the nanowebs against *Staphylococcus aureus* bacteria was determined according to ASTM E2149-10 standard.

Statistics. All data regarding diameter and mechanical properties were expressed as mean ± standard deviation. Differences between samples were analyzed by investigation of analysis of variance (ANOVA-SPSS 21.0) at 0.05 significance level.

Results and discussion

FTIR spectroscopy

FTIR spectroscopy was used to confirm the successful functionalization of CNTs and to compare the spectral differences between pure PAN and PAN/PANI composite nanowebs.

KBr pellets were prepared to characterize the amine-functionalized CNTs. Peak positions of the functionalized CNTs can be seen in Figure 2 in comparison with that of the pristine CNTs.

In comparison with pristine CNTs, new peaks appeared in the spectra of CNT–NH_2. Region 3500–3400 cm^{-1} can be attributed to –OH and N–H stretching vibrations.[2] The peak at 1630 cm^{-1} was assigned to C=C stretching of CNT structure and C=O stretching of amide (–NH–C=O) structure. The peaks at 1540 cm^{-1} and 1140 cm^{-1} were attributed to C–NH, C=N, and C–C stretching vibrations, respectively. The peak at 620 cm^{-1} showed the amide structure N–C=O.[28]

The FTIR spectra of PAN nanofibers and PAN/PANI composite nanofibers are presented in Figure 3. Pure PAN nanofibers displayed the characteristic absorption peaks of nitrile (–C≡N) group at around 2240 cm^{-1}. Also methylene (CH_2) group of PAN showed a series of characteristic bands in the regions from 2930 to 2870 cm^{-1}, from 1460 to 1450 cm^{-1}, and from 1380 to 1360 cm^{-1}.[23,28] In the FTIR spectra of PAN/PANI composite nanofibers, in addition to the characteristic peaks of pure PAN, a wide peak was observed at around 3400 cm^{-1}, which was due to the free imine (–NH) group of PANI. Also a peak was observed at around 3280 cm^{-1} attributed to the aromatic C–H strecthing of PANI. Another peak centered at 1730 cm^{-1} originated from the carbonyl (–C=O) groups in the CSA.[23]

Morphological properties

SEM images taken with 10 k × magnification are presented in Figure 4, while the average nanofiber diameters are presented in Table 2 with standard deviation values and graphically in Figure 5. Pure PAN nanofibers and composite nanofibers were uniform in structure.

The additives such as CNTs, silver nanoparticles, and PANI can promote two opposite effects on the

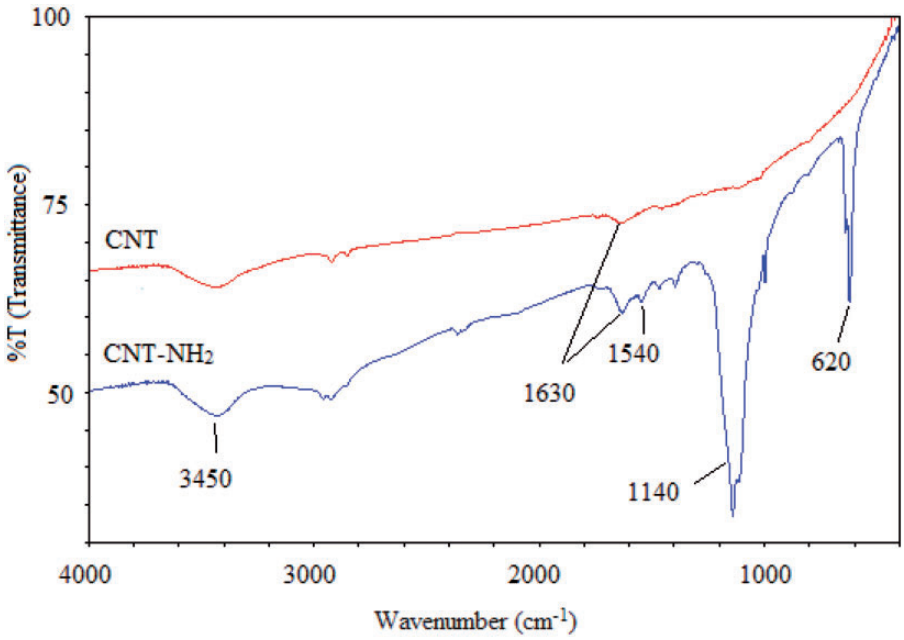

Figure 2. FTIR spectra of pristine and amine-functionalized carbon nanotubes.

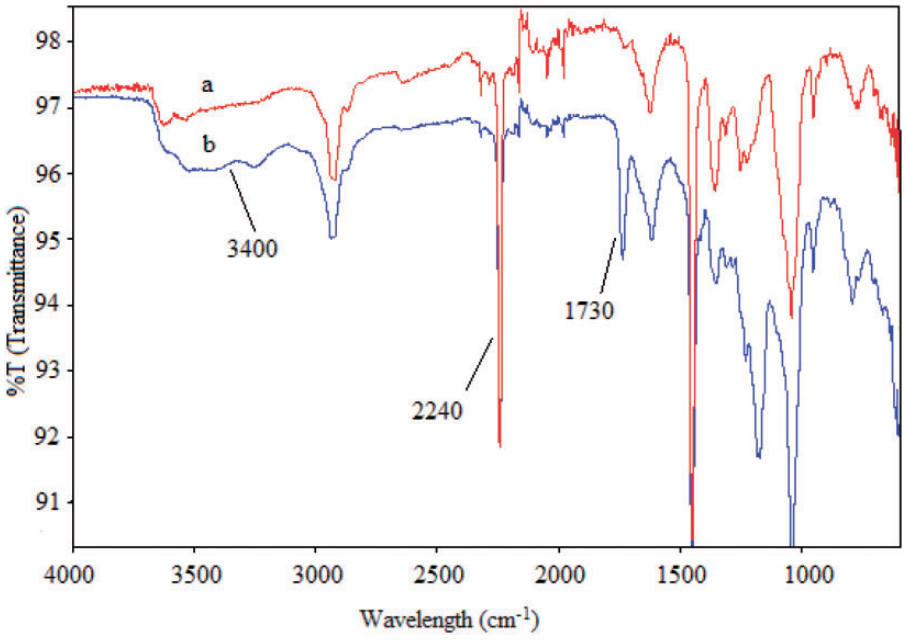

Figure 3. FTIR spectra of (a) PAN-ref and (b) PAN–PANI nanofibers.

nanofiber formation and diameter. They may increase the viscosity due to the increased substance concentration and result in larger nanofiber diameter or they may decrease the diameter of nanofiber due to an increased charge density leading to higher elongation of nanofiber during electrospinning.[29,30] Thus, the diameter of nanofibers mostly depends on the phenomenon that is dominant. In our case, increase in the diameter of the samples with PANI was more pronounced than the others as can be seen from Table 2. This might have been due to the higher viscosity of the electrospinning solution. The viscosity was measured as 820 mPa/s for PAN/PANI and 500 mPa/s for PAN–3CNT. Higher diameter of samples with PANI might have also been due to the longer drying time of nanofibers with PANI, since it was observed that nanofiber web with PANI

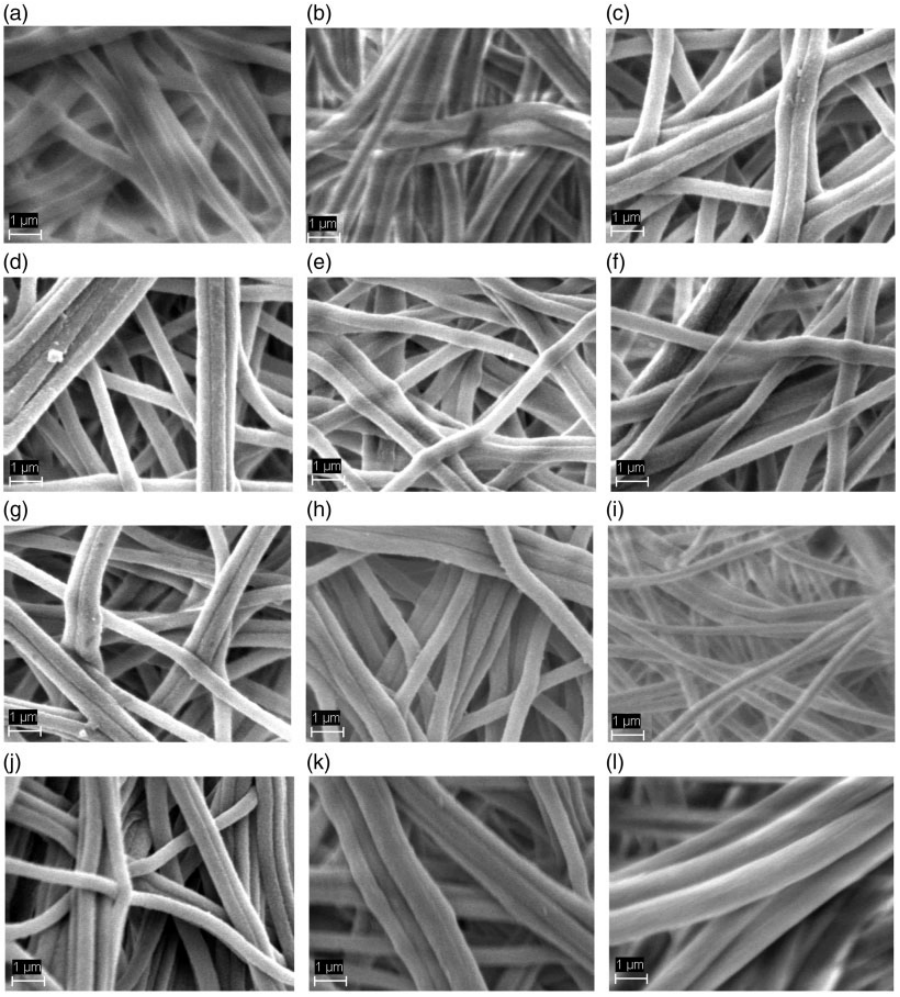

Figure 4. SEM images of (a) PAN-ref, (b) PAN–PANI, (c) PAN–1CNT, (d) PAN–3CNT, (e) PAN–PANI–1CNT, (f) PAN–PANI–3CNT, (g) PAN–1$AgNO_3$–R, (h) PAN–3$AgNO_3$–R, (i) PAN–PANI–1$AgNO_3$–R, (j) PAN–PANI–3$AgNO_3$–R, (k) PAN–1CNT–1$AgNO_3$–R, (l) PAN–PANI–1CNT–1$AgNO_3$–R nanofibers.

Table 2. Diameters of composite nanofibers.

Sample	Diameter (nm)
PAN-ref	515 ± 72.1
PAN–PANI	575 ± 86.2
PAN–1CNT	536 ± 91.1
PAN–3CNT	531 ± 74.3
PAN–PANI–1CNT	556 ± 77.8
PAN–PANI–3CNT	719 ± 122.2
PAN–1$AgNO_3$–R	491 ± 82
PAN–3$AgNO_3$–R	413 ± 61
PAN–PANI–1$AgNO_3$–R	410 ± 56
PAN–PANI–3$AgNO_3$–R	491 ± 84
PAN–1CNT–1$AgNO_3$–R	559 ± 60.26
PAN–PANI–1CNT–1$AgNO_3$–R	864 ± 112.47

Note: CNT: carbon nanotube; PANI: polyaniline; $AgNO_3$: silver nitrate; PAN: polyacrylonitrile.

was damper than the samples without PANI after the electrospinning process. Samples containing $AgNO_3$ or PANI + $AgNO_3$ had smaller diameters than those containing CNT or PANI + CNT. This might have been due to the reduction of $AgNO_3$ into silver nanoparticles by hydrazinium hydroxide and the diffusion of metallic silver atoms into the inner parts of the nanofibers forming coordination bonds with nitrile (C≡N) groups. It is reported that formation of coordination bonds between silver atoms and nitrile groups of PAN causes homogeneous distribution of silver nanoparticles in nanofiber web, thus decreasing the agglomeration tendency.[31] Nanofibers, which contained PAN + PANI + $AgNO_3$, were thinner than the nanofibers, which contained PAN + PANI + CNT. Higher charge density might have also been effective on this result. An increase in the amount and type of additives generally resulted in an increase in diameter due to the presence of higher amount of substance, increased viscosity, and the

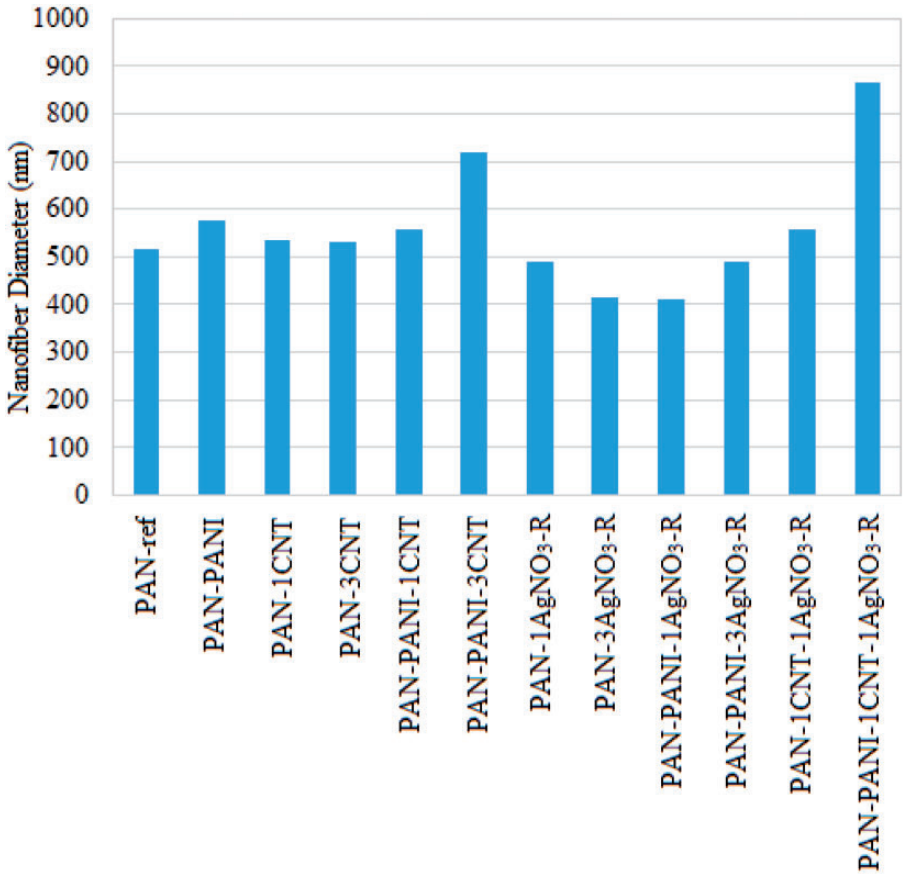

Figure 5. Average nanofiber diameters of reference and composite nanofibers.

tendency of agglomeration. PAN–PANI–1CNT–1$AgNO_3$ sample had the largest diameter (Table 2). ANOVA statistical analysis showed that the differences between PAN–PANI, PAN–PANI–3CNT, PAN–PANI–1$AgNO_3$–R, PAN–PANI–1CNT–1$AgNO_3$–R, and PAN-ref were statistically significance at 0.05 significance level.

Analysis of mechanical properties

The mechanical properties of nanofiber webs are presented in Table 3, while the breaking strength values are graphically represented in Figure 6. The mechanical properties of electrospun nanofiber webs are closely related to the geometric arrangement of nanofibers, the bonding structure among the fibers, distribution of nanofibers and pores between the nanofibers, existence of imperfections, flaws and branching of the nanofibers, structure and distribution of the additives, etc.[32,33] PANI slightly improved the strength of PAN–CNT composite nanofiber when the nano particle (CNT) amount was not more than 1 wt%. This might have been due to the higher crystallinity in the presence of PANI (Table 5 and Figure 7) leading to an increase in breaking strength. As can be seen from the results, there is a tendency of a decrease in breaking strength of composite nanofibers as the amount and types of additives increased due to the increase in agglomeration tendency. Thus, while PAN–PANI–1CNT had higher breaking strength than PAN–1CNT sample, PAN–PANI–3CNT had lower breaking strength than PAN–3CNT due to the increase in the content and additive type leading to an increase in agglomeration. Samples with $AgNO_3$ had higher breaking strength than the samples with CNT in connection with the homogeneous distribution of silver nanoparticles ($AgNO_3$) in nanofiber web via reduction by hydrazinium hydroxide.[28] Besides, hydrazinium hydroxide might have also caused to the formation of crosslinks between the polymer chains leading to increased tensile strength.[34] The highest breaking strength values were obtained for the samples of PAN–PANI–1$AgNO_3$–R and PAN–1$AgNO_3$–R, which showed an improvement in breaking strength approximately 60% compared to PAN-reference together with an improvement in breaking strain. The differences between the strength values of PAN–1$AgNO_3$–R, PAN–PANI–1$AgNO_3$–R and PAN-ref were statistically significant at 0.05 significance level

Table 3. Mechanical properties of composite nanofibers.

Samples	Breaking strength MPa	Breaking elongation %	E-modulus MPa
PAN-ref	8.64 ± 3.1	9.0 ± 2.7	10.6 ± 36.5
PAN–PANI	8.61 ± 1.1	73.4 ± 5.2	59.2 ± 17.1
PAN–1CNT	8.99 ± 2.0	9.7 ± 2.7	38.2 ± 17.8
PAN–3CNT	9.35 ± 1.2	14 ± 2.4	95.7 ± 36.0
PAN–PANI–1CNT	10.8 ± 3.1	14.2 ± 5.12	87.3 ± 33.1
PAN–PANI–3CNT	5.76 ± 1.7	65.4 ± 11.5	41.8 ± 14.0
PAN–1$AgNO_3$–R	13.8 ± 2.4	36.4 ± 5.7	73.0 ± 29
PAN–3$AgNO_3$–R	11.2 ± 3.1	18.7 ± 6.4	39.2 ± 13.1
PAN–PANI–1$AgNO_3$–R	13.9 ± 2.2	7.0 ± 1.5	166.6 ± 53.12
PAN–PANI–3$AgNO_3$–R	9.3 ± 2.3	7.6 ± 2.5	132.1 ± 30
PAN–1CNT–1$AgNO_3$–R	6.8 ± 1.23	11.8 ± 3.4	31.1 ± 9.3
PAN–PANI–1CNT–1$AgNO_3$–R	7.1 ± 1.1	11.8 ± 1.0	36.4 ± 12.1

Note: CNT: carbon nanotube; PANI: polyaniline; $AgNO_3$: silver nitrate; PAN: polyacrylonitrile.

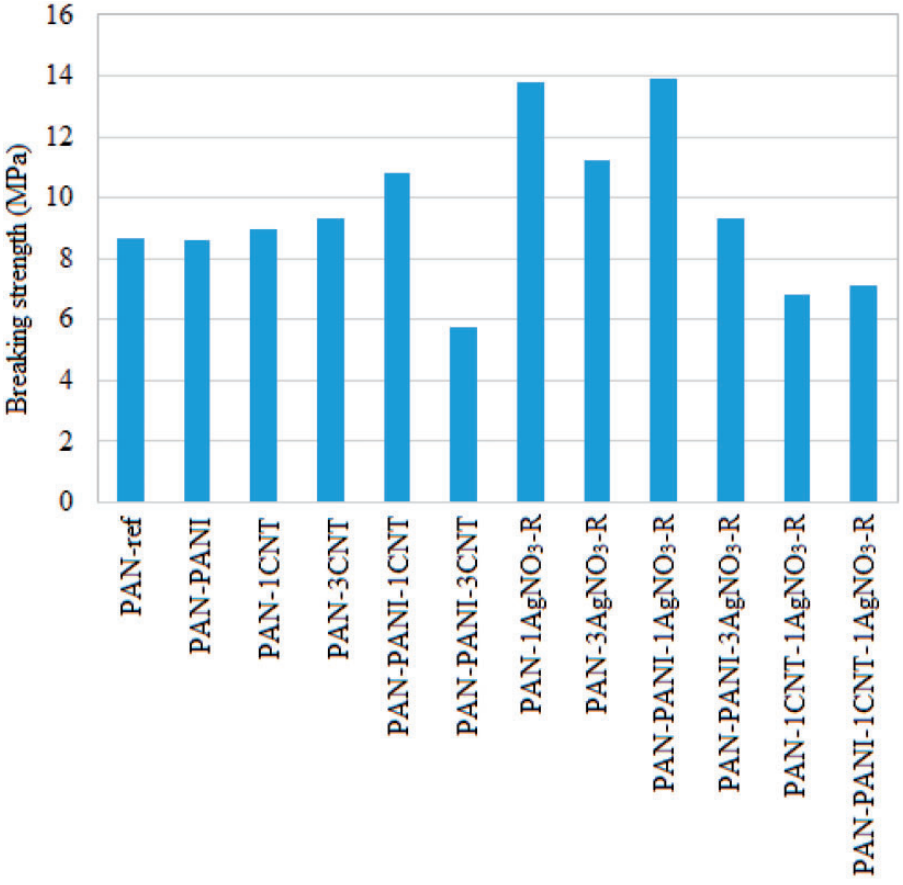

Figure 6. Average breaking strength values of reference and composite nanofiber webs.

according to ANOVA. The analysis of breaking elongation and the tensile modulus of the composite nanofiber is very complex, since polymeric nanofiber webs do not behave as the metallic rods. There are very complex interactions between the uncontrollable parameters such as the orientation of the nanofibers, the placement of nanofibers in the nanoweb, pore size, and distribution through the nanofiber web.[32,35]

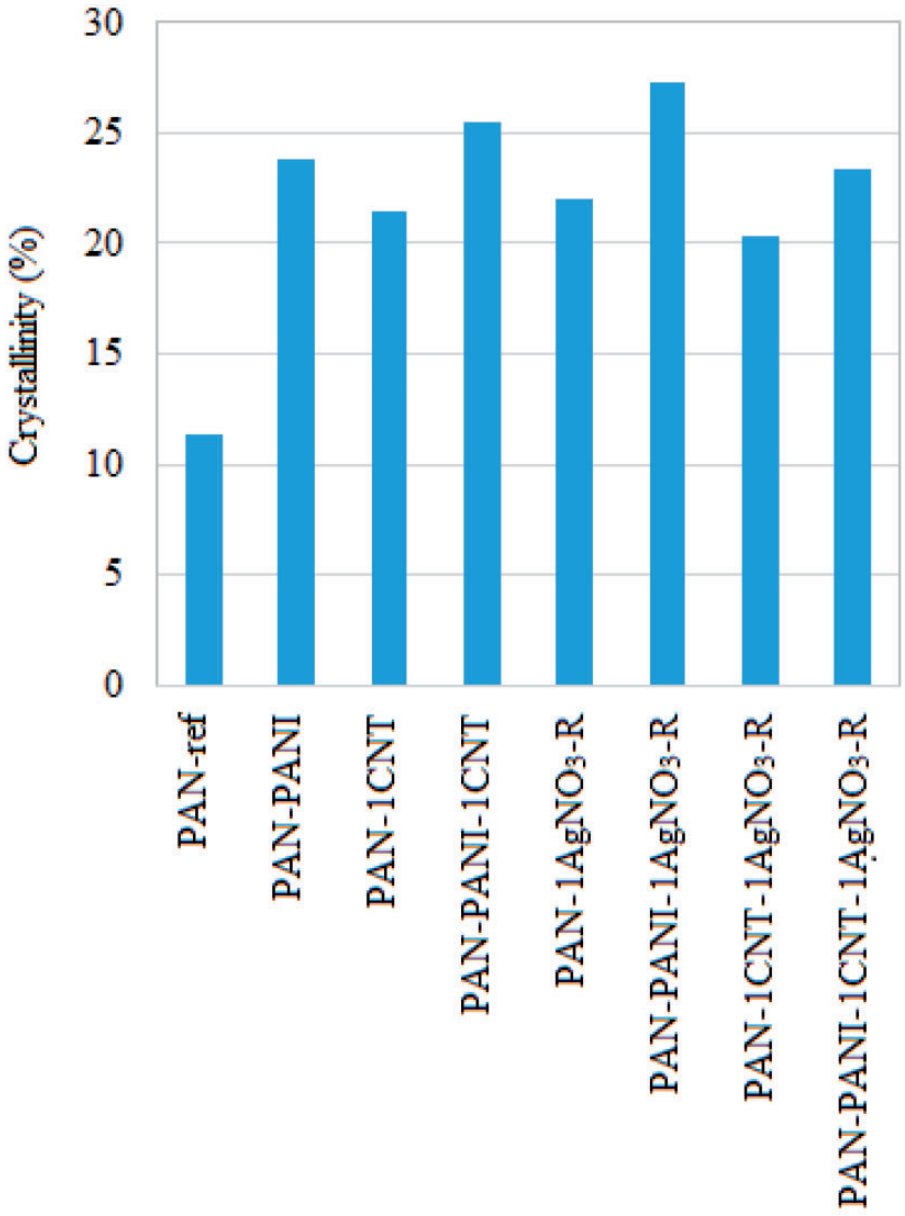

Figure 7. Crystallinity values (%) of reference and composite nanowebs.

Electrical conductivity of composite nanofibers

The highest electrical conductivity value of 10^{-6} S/cm was obtained from the sample of PAN–PANI (Table 4). As known, reduced $AgNO_3$ and CNT have also electrical conductivity properties. As seen from Table 4, PAN–$AgNO_3$ composite structures had 10^{-8} S/cm electrical conductivity. However, PAN–PANI–$AgNO_3$ had 10^{-7} S/cm electrical conductivity. This improvement is because of the addition of PANI. PAN–CNT composite structure had an electrical conductivity of 10^{-8} S/cm. However, PAN–1CNT–1$AgNO_3$ (1% CNT, 1% $AgNO_3$) had an electrical conductivity of 10^{-7} S/cm. This is because of the improvement in conductive network by using low amount of CNT (1%).

As the filler type and content increased, the conductivity decreased due to the possible agglomeration and disruption of the conductive network. Thus, PAN–PANI samples containing 3% CNT (PAN–PANI–3CNT) or PAN–PANI–1CNT–1$AgNO_3$ showed lower electrical conductivity (10^{-8} or 10^{-9} S/cm) than PAN–PANI due to the increase in the content and filler type resulting in the increase in agglomeration and disruption of conductive network.

Second highest conductivity value was obtained from the sample containing $AgNO_3$ and PANI (10^{-7} S/cm) which is in the range of semiconductive

materials.[36] Generally, samples containing CNT showed lower conductivity (around 10^{-8} S/cm, 10^{-9} S/cm) than the samples containing $AgNO_3$, which was still in the range of antistatic materials.

X-ray diffraction

The crystallinity values (%) and peak positions are presented in Table 5, while the crystallinity values are graphically presented in Figure 7 and equatorial XRD traces are presented in Figure 8. The XRD traces and crystallinity values appeared to be influenced by the incorporation of the additives. The peak appeared at 2θ value of 38°, which corresponded to the (111) plane of silver confirmed the formation of silver nanoparticles in the nanofiber structure for the samples containing $AgNO_3$.[19] Main characteristic peaks of PANI, which are reported to occur at $2\theta = 15.07°$, 20.22°, and 25.18°[37] were observed for the samples that contained PANI. Crystallinity of PAN-ref was found to be 11.3%. All the other samples showed higher crystallinity values than PAN-ref, which varied between 20% and 27% (Table 5 and Figure 7). The incorporation of CNTs, AgNPs, and PANI caused an increase in the crystallinity of PAN-ref due to nucleating effect of the additives[38,39] and long, rigid PANI chains.[40] Generally, it was found that PANI improved the crystallinity more than the CNTs and AgNPs. PANI polymer chains are long, rigid, and contain aromatic rings leading to an increase in the crystallinity of PAN chains. PANI might have also caused an improvement in the alignment and orientation of macromolecules in the nanofibers due to the increased conductivity of polymer solution jet during electrospinning. Another reason for the improvement in the crystallinity of samples, which contained PANI may be the slow drying

Table 4. Electrical conductivity of the composite nanofibers.

Sample	Conductivity (S/cm)
PAN–PANI	$1.07 \times 10^{-6} \pm 4.22 \times 10^{-7}$
PAN–1CNT	$2.80 \times 10^{-8} \pm 3.9 \times 10^{-9}$
PAN–3CNT	$2.10 \times 10^{-8} \pm 7.8 \times 10^{-9}$
PAN–PANI–1CNT	$3.07 \times 10^{-8} \pm 1.1 \times 10^{-8}$
PAN–PANI–3CNT	$3.89 \times 10^{-9} \pm 1.2 \times 10^{-9}$
PAN–1$AgNO_3$	$4.56 \times 10^{-8} \pm 1.53 \times 10^{-8}$
PAN–3$AgNO_3$	$3.79 \times 10^{-8} \pm 1.12 \times 10^{-8}$
PAN–PANI–1$AgNO_3$	$1.47 \times 10^{-7} \pm 5.64 \times 10^{-8}$
PAN–PANI–3$AgNO_3$	$1.3 \times 10^{-7} \pm 3.66 \times 10^{-8}$
PAN–1CNT–1$AgNO_3$	$4.02 \times 10^{-7} \pm 6.88 \times 10^{-8}$
PAN–PANI–1CNT–1AgNO3	$1.23 \times 10^{-8} \pm 1.15 \times 10^{-9}$

Note: CNT: carbon nanotube; PANI: polyaniline; $AgNO_3$: silver nitrate; PAN: polyacrylonitrile.

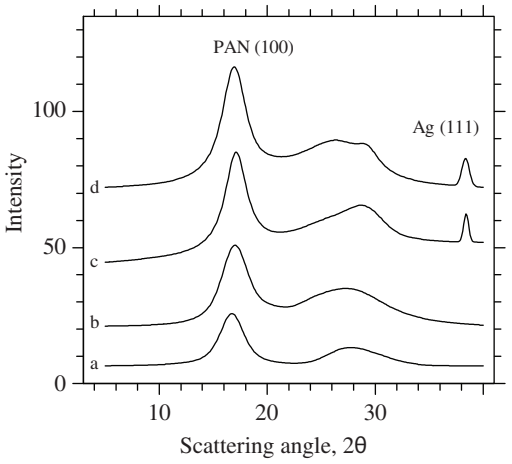

Figure 8. Equatorial X-ray diffraction traces of (a) PAN-ref, (b) PAN–PANI, (c) PAN–1CNT–1$AgNO_3$–R, (d) PAN–PANI–1CNT–1$AgNO_3$–R.

Table 5. XRD results of composite nanofibers.

Sample	Crystallinity (%)	PAN (100) (°2θ)	PAN disordered (°2θ)	PAN (110) (°2θ)	CNT (002)	Ag (111)	PANI Peak-1 (°2θ)	PANI Peak-2 (°2θ)	PANI Peak-3 (°2θ)
PAN-ref	11.3	16.70	26.60	29.20	–		–	–	–
PAN–PANI	23.8	16.97	26.66	29.3	–		15.1 (broad)	20.0 (broad)	24.0 (broad)
PAN–1CNT	21.5	17.04	–	29.2	26.5		–	–	–
PAN–PANI–1CNT	25.5	16.97	–	29.2	26.5		15.1 (broad)	20.0 (broad)	24.0 (broad)
PAN–1$AgNO_3$–R	22.0	17.07	26.68	29.2	–	38.3	–	–	–
PAN–PANI–1$AgNO_3$–R	27.3	17.10	26.66	29.3	–	38.4	15.1 (broad)	20.0 (broad)	24.0 (broad)
PAN–1CNT–1$AgNO_3$–R	20.3	17.11	–	29.2	26.5	38.4	–	–	–
PAN–PANI–1CNT–1$AgNO_3$–R	23.4	17.04	–	29.2	26.5	38.37	15.1 (broad)	20.0 (broad)	24.0 (broad)

Note: CNT: carbon nanotube; PANI: polyaniline; $AgNO_3$: silver nitrate; PAN: polyacrylonitrile.

of the samples. As it is very well known, the electrospinnning is a fast drying process generally retarding the development of crystallinity.[39]

The addition of AgNPs resulted in a slightly higher crystallinity values than the addition of CNTs. Pristine multi-walled CNTs we used in this study are reported to be 60–100 nm in diameter and 5–15 μm in length on the material data sheet and with the amine groups attached onto their walls, they become bulkier after amine functionalization. On the other hand, the size of the silver nanoparticles, which is obtained with the applied method, is reported to be between 40 and 100 nm in literature and also one of our previous studies.[19,31] Thus, CNTs are bigger in size than AgNPs. The bulky nature of CNT–NH_2 structure might have kept the polymer chains apart from each other and inhibited the crystallization of PAN polymer chains. When the polymer chains are unable to approach each other, crystallization becomes difficult to achieve. The highest crystalinity was obtained from the sample of PAN–PANI–$AgNO_3$.

Thermal analysis

DSC results of composite nanofibers in the range of 40–400°C are presented in Table 6. As can be seen from Table 6, additives of PANI, AgNPs, and CNTs generally resulted in an increase in cyclization temperature (T_c). Increased cyclization temperature means that the cyclization reactions in the presence of additives such as PANI, CNTs, and AgNPs require higher temperature to take place, leading to more stable thermal structure.

As the nanofillers content increased from 1% to 3%, the enthalpy was found to decrease. Higher amount of nanofillers in the composite structure facilitates the agglomeration tendency and this might have resulted in a decrease in the cyclization energy. Although composite nanofiber of PAN–PANI had the lowest cyclization energy, presence of PANI in composite structure together with other additives such as AgNPs and CNTs resulted in an increase in cyclization energy (ΔH), which meant that the whole system required more energy for cyclization.

The results presented in Table 6 demonstrated that the presence of AgNPs increased the cyclization energy. The contribution of AgNPs on the formation of crystalline structures arises from their ability to coordinate with the nitrile groups of PAN. When Ag ions and nitrogen atom of nitrile groups form coordination bonds, the resulting structure is reported to contain certain amount of graphitic structure as demonstrated by Raman spectra.[33] The presence of isolated graphite structure in the presence of AgNPs might have caused an increase in the cyclization energy (Table 6). The reaction between Ag nanoparticles and nitrile groups is likely to result, at room temperature, in the dehydrogenation reactions causing the formation of C=C double bonds when Ag nanoparticles act as a catalyst for such coordination reactions.

Table 6. Cyclization temperatures and enthalpy values of nanofibers.

Samples	T_c (°C)	ΔH (j/g)
PAN-ref	303.40	437.7
PAN–PANI	330.62	293.2
PAN–1CNT	320.04	430.2
PAN–3CNT	324.54	273.3
PAN–PANI–1CNT	323.25	516.2
PAN–PANI–3CNT	304.32	349.7
PAN–1$AgNO_3$–R	314.11	451.6
PAN–3$AgNO_3$–R	321.83	339.0
PAN–PANI–1$AgNO_3$–R	325.63	491.4
PAN–PANI–3$AgNO_3$–R	322.26	459.4
PAN–1CNT–1$AgNO_3$–R	322.48	457.3
PAN–PANI–1CNT–1$AgNO_3$–R	325.43	518.4

Note: CNT: carbon nanotube; PANI: polyaniline; $AgNO_3$: silver nitrate; PAN: polyacrylonitrile.

Antimicrobial efficiency

Antimicrobial efficiency test results of composite nanofibers are presented in Table 7. According to FTTS-FA-002 standard, samples with 99% or over 99% antimicrobial efficiency are called as antimicrobial material.[41]

While pure PAN nanofiber does not show antimicrobial effect,[42] most of the nanoparticles can have antimicrobial effect due to their large surface area.[43] CNTs have weak antimicrobial properties,[44] while AgNPs show excellent antimicrobial properties. The amount

Table 7. Antimicrobial efficiency of nanofibers.

Samples	Antimicrobial efficiency
PAN ref	−
PAN–PANI	−
PAN–1CNT	−
PAN–PANI–1CNT	−
PAN–1$AgNO_3$–R	−
PAN–3$AgNO_3$–R	+
PAN–PANI–1$AgNO_3$–R	+
PAN–1CNT–1$AgNO_3$–R	+

Note: CNT: carbon nanotube; PANI: polyaniline; $AgNO_3$: silver nitrate; PAN: polyacrylonitrile.
(−) Represent not enough antimicrobial activity; (+) represent antimicrobial activity.

of antimicrobial active material in the sample is important for the antimicrobial efficiency. While nanofibers with 1% $AgNO_3$ was unable to provide enough antimicrobial effect due to low concentration, nanofibers with 3% $AgNO_3$ provided sufficient antimicrobial effect. PANI may also behave as antimicrobial material due to its surface hydrophilicity, electrostatic adsorption between PANI and bacteria, higher molecular weight, and direct contact between polymer material and bacterial cells.[43] Interactions between nanoparticles and PANI provided better antimicrobial effect. Although PANI or nanoparticles with low concentrations (PAN–1CNT and PAN–1$AgNO_3$–R) could not provide enough antimicrobial effect, when they are used together, the composite material (PAN–PANI–1$AgNO_3$–R and PAN–1CNT–1$AgNO_3$–R) gained antimicrobial properties due to the synergistic effect of the additives.

The synergistic effect may be caused by the interactions between the additives, which might have formed during the preparation of the electrospinning solutions and changed the morphology of the nanofibers. For example, PANI is reported to be effective in stabilizing particles against aggregation. Smaller AgNPs having larger surface area would have given higher bactericidal effect than larger AgNPs.[43,45] Besides, the fiber structure becoming more porous with the addition of different types of the additives might have led to the higher release of the silver ions resulting in higher antibacterial efficiency.

Conclusions

This study was carried out to determine what kind of synergistic effect occurs when more than one additive (CNT, AgNPs, PANI) was used together during the production of composite nanofiber. While many important results were explained in the Results and discussion section, some important conclusions have also been pointed out in the following.

1. Increase in the amount and types of additives generally resulted in an increase in the diameter of nanofibers and decrease in mechanical strength.
2. Increase in the diameter of the samples with PANI is higher than the others and samples containing AgNPs have smaller diameter than the nanofibers containing CNTs.
3. Samples containing AgNPs showed higher breaking strength and electrical conductivity than the samples containing CNTs whose electrical conductivity was still in the range of antistatic materials compared to insulator PAN reference.
4. All of the composite nanofiber samples showed higher crystallinity than pure PAN nanofiber (PAN-ref). Generally, PANI improved the crystallinity more than the nanoparticles (CNT, AgNPs) and AgNPs provided slightly higher crystallinity than CNTs.
5. As the nanofillers ratio increased from 1% to 3%, the enthalpy for cyclization decreased; however, the use of the additives (PANI, CNT, AgNPs) at low concentration resulted in an increase in the temperature and enthalpy for cyclization compared to pure PAN nanofiber (PAN-ref).
6. While no antimicrobial activity was observed at low concentration of each of the additives (PANI, CNT, AgNPs), the composite materials of PAN–PANI–1$AgNO_3$ and PAN–1CNT–1$AgNO_3$ showed antimicrobial properties due to the synergistic effect of the additives.

When all the properties of the composite samples are considered, it can be said that the composite PAN nanofibers with 3 wt% PANI and 1 wt% $AgNO_3$ (PAN–PANI–1$AgNO_3$) generally presented better performance compared to others, especially for electrical conductivity (semiconductive material applications), antimicrobial activity, mechanical strength, crystallization, and thermal stability.

Conflict of interest

The author(s) declared no potential conflicts of interest with respect to the research, authorship, and/or publication of this article.

Funding

The author(s) disclosed receipt of the following financial support for the research, authorship, and/or publication of this article: We would like to thank to TUBITAK for supporting this study (Project 112M877).

References

1. Nataraj SK, Yang KS and Aminabhavi TM. Polyacrylonitrile-based nanofibers—a state-of-the-art review. *Prog Polym Sci* 2012; 37: 487–513.
2. Oueiny C, Berlioz S and Perrin F. Carbon nanotubes-polyaniline composites. *Prog Polym Sci* 2014; 39: 707–748.
3. Barra GMO, Leyva ME, Soares BG, et al. Electrically conductive, melt-processed polyaniline/EVA blends. *J Appl Polym Sci* 2001; 82: 114–123.
4. Yang CY, Cao Y, Smith P, et al. Morphology of conductive, solution-processed blends of polyaniline and poly(methyl methacrylate). *Synth Met* 1993; 53: 293–301.
5. Paul RK and Pillai CK. Melt/solution processable polyaniline with functionalized phosphate ester dopants and its thermoplastic blends. *J Appl Polym Sci* 2001; 80: 1354–1367.
6. Barra GMO, Leyva ME, Soares BG, et al. Solution-cast blends of polyaniline-DBSA with EVA copolymers. *Synth Met* 2002; 130: 239–245.

7. Pan W, Zhang Q and Chen Y. Characterization of PAN/PANI-DBSA blend nanofibers produced by electrospinning method. *Optoelec Adv Mater Rapid Commun* 2010; 4: 2118–2122.
8. Li M, Guo Y, Wei Y, et al. Electrospinning polyaniline-contained gelatin nanofibers for tissue engineering applications. *Biomaterials* 2006; 27: 2705–2715.
9. Chen D, Guo X, Wang Z, et al. Polyaniline nanofiber gas sensors by direct-write electrospinning. In: *Micro Electro Mechanical Systems (MEMS), 2011 IEEE 24th international conference*, Cancun, Mexico, 23–27 January 2011, pp. 1369–1372. DOI: 10.1109/MEMSYS.2011.5734689
10. Picciani PHS, Medeiros ES, Pan Z, et al. Development of conducting polyaniline/poly (lactic acid) nanofibers by electrospinning. *J Appl Polym Sci* 2009; 112: 744–753.
11. Hou H, Ge JJ, Zeng J, et al. Electrospun polyacrylonitrile nanofibers containing a high concentration of well-aligned multiwall carbon nanotubes. *Chem Mater* 2005; 17: 967–973.
12. Wang X, Si Y, Wang X, et al. Tuning hierarchically aligned structures for high-strength PMIA–MWCNT hybrid nanofibers. *Nanoscale* 2013; 5: 886–889.
13. Brancato V, Visco AM, Pisyone A, et al. Effect of functional groups of multi-walled carbon nanotubes on the mechanical, thermal and electrical performance of epoxy resin based nanocomposites. *Journal of Composite Materials* 2013; 47: 3091–3103.
14. Ucar N, Demirsoy N, Onen A, et al. The effect of reduction methods and stabilizer (PVP) on the properties of polyacrylonitrile (PAN) composite nanofibers in the presence of nanosilver. *J Mater Sci* 2015; 50: 1855–1864.
15. Qiao B, Ding X, Hou X, et al. Study on the electrospun CNTs/polyacrylonitrile-based nanofiber composites. *J Nanomater* 2011; 2011: 839462.
16. Park OK, Lee S, Joh HI, et al. Effect of functional groups of carbon nanotubes on the cyclization mechanism of polyacrylonitrile (PAN). *Polymer* 2012; 53: 2168–2174.
17. Wang K, Gua M, Wangi JJ, et al. Functionalized carbon nanotube/polyacrylonitrile composite nanofibers: fabrication and properties. *Polym Adv Technol* 2012; 23: 262–271.
18. Shi Q, Vitchuli N, Nowak J, et al. Durable antibacterial Ag/polyacrylonitrile (Ag/PAN) hybrid nanofibers prepared by atmospheric plasma treatment and electrospinning. *Eur Polym J* 2011; 42: 1402–1409.
19. Sichani GN, Morshed M, Amirnasr M, et al. In situ preparation, electrospinning, and characterization of polyacrylonitrile nanofibers containing silver nanoparticles. *J Appl Polym Sci* 2010; 116: 1021–1029.
20. Pan W, He X and Chen Y. Preparation and characterization of polyacrylonitrile-polyaniline blend nanofibers. *Appl Mech Mater* 2011; 44–47: 2195–2198.
21. Gao C, Vo DC, Jin ZY, et al. Multihydroxy polymer-functionalized carbon nanotubes: synthesis, derivatization, and metal loading. *Macromolecules* 2005; 38: 8634–8648.
22. Zhao Z, Yang Z, Hu Y, et al. Multiple functionalization of multi-walled carbon nanotubes with carboxyl and amino groups. *Appl Surf Sci* 2013; 276: 476–481.
23. Kizildag N, Ucar N, Onen A, et al. The effect of the dissolution process and the polyaniline content on the properties of polyacrylonitrile–polyaniline composite nanoweb. *J Ind Text*, Epub ahead of print, 16 December 2014. DOI: 10.1177/1528083714564636
24. Demirsoy N, Ucar N, Onen A, et al. The effect of dispersion technique, silver particle loading, and reduction method on the properties of polyacrylonitrile-silver composite nanofiber. *J Ind Text*, Epub ahead of print, 2 October 2014. DOI: 10.1177/1528083714553690
25. ASTM International, D257-07. Standard test methods for DC resistance or conductance of insulating materials. Available at: http://www.astm.org/DATABASE.CART/HISTORICAL/D257-07.htm.
26. ASTM International, D4496-13. Standard test method for DC resistance or conductance of moderately conductive materials. Available at: http://www.astm.org/Standards/D4496.htm.
27. Hindeleh AM and Johnson DJ. Crystallinity and crystallite size measurement in polyamide and polyester fibres. *Polymer* 1978; 19: 27–32.
28. Prestsch E, Bühlmann P and Affolter C. Structure determination of organic compounds, Tables of spectral data. New York, NY: Springer, 2000.
29. Heikkilä P and Harlin A. Electrospinning of polyacrylonitrile (PAN) solution: effect of conductive additive and filler on the process. *eXPRESS Polym Lett* 2009; 3: 437–445.
30. Wang N, Si Y, Wang N, et al. Multilevel structured polyacrylonitrile/silica nanofibrous membranes for high-performance air filtration. *Sep Purif Technol* 2014; 126: 44–51.
31. Wang Y, Yang Q, Shan G, et al. Preparation of silver nanoparticles dispersed in polyacrylonitrile nanofiber film spun by electrospinning. *Mater Lett* 2005; 59: 3046–3049.
32. Andrady AL. Science and technology of polymer nanofibers. Hoboken, NJ: John Wiley, 2008.
33. Wang J, Li Y, Tian H, et al. Waterproof and breathable membranes of waterborne fluorinated polyurethane modified electrospun polyacrylonitrile fibers. *RSC Adv* 2014; 4: 61068–61076.
34. Shoushtari AM, Zargaran M and Abdous M. Preparation and characterization of high efficiency ion-exchange crosslinked acrylic fibers. *J App Poly Sci* 2006; 101: 2202–2209.
35. Ucar N, Ayaz O, Bahar E, et al. Thermal and mechanical properties of composite nanofiber webs and films containing cellulose nanowhiskers. *Text Res J*, Epub ahead of print 26 June 2012. DOI: 10.1177/0040517512450761
36. Almuhamed S, Khenoussi N, Schacher L, et al. Measuring of electrical properties of MWNT-reinforced PAN nanocomposites. *J Nanomater* 2012; 2012: 1–7.
37. Qiao H, Chen F, Xia X, et al. Characterization of polyaniline/Fe_3O_4-polyacrylonitrile composite nanofibers. *J Fiber Bioeng Inf* 2010; 2: 253–258.
38. Avalos-Belmontes F, Ramos-deValle LF, Ramírez-Vargas E, et al. Nucleating effect of carbon nanoparticles and their influence on the thermal and chemical stability of polypropylene. *J Nanomater* 2012; 2012: 406214.

39. Bahar E, Ucar N, Onen A, et al. Thermal and mechanical properties of polypropylene nanocomposite materials reinforced with cellulose nano whiskers. *J Appl Polym Sci* 2012; 125: 2882–2889.
40. Kamali M, Ghorashi SAA and Asadollahi MA. Controllable synthesis of silver nanoparticles using citrate as complexing agent: characterization of nanoparticles and effect of pH on size and crystallinity. *Iran J Chem Chem Eng* 2012; 31: 21–28.
41. FTTS-FA-002. Antibacterial textiles for medical use standards. *Specified Requirements of Antibacterial Textiles for Medical Use*. Available at: http://www.ftts.org.tw/images/fa002E.pdf.
42. Song R, Yan J, Xu S, et al. Silver ions/ovalbumin films layer-by-layer self-assembled polyacrylonitrile nanofibrous mats and their antibacterial activity. *Colloid Surface B* 2013; 108: 322–328.
43. Boomi P, Prabu HG and Mathiyarasu J. Synthesis, characterization and antibacterial activity of polyaniline/Pt-Pd nanocomposite. *Eur J Med Chem* 2014; 72: 18–25.
44. Qi X, Gunawan P, Xu R, et al. Cefalexin-immobilized multi-walled carbon nanotubes show strong antimicrobial and anti-adhesion properties. *Chem Eng Sci* 2012; 84: 552–556.
45. Jia Q, Shan S, Jiang L, et al. Synergistic antimicrobial effects of polyaniline combined with silver nanoparticles. *J Appl Polym Sci* 2012; 125: 3560–3566.